TAU-THEORY-BASED VISUAL CUEING METHOD FOR OBSTACLE AVOIDANCE

Ceren Cansu Esmek
Graduate Student

Rahul Tauro-Padival
Undergraduate Student

Karen M. Feigh
Professor

J.V.R. Prasad
Professor

Vertical Lift Research Center of Excellence
Georgia Institute of Technology
Atlanta, GA, U.S.

ABSTRACT

Low situational awareness (SA) when operating close to terrain and obstacles significantly increases risk by dramatically reducing reaction times. This study aims to facilitate real-time trajectory adjustments and improve pilot SA without increasing cognitive load by focusing on the specific challenge of maneuvering around obstacles in hostile and degraded visual environments (DVE). This methodology is intended to improve the safety and efficiency of low-altitude rotorcraft missions. In addition to the bank angle cueing methodology, this study proposes a deceleration and rate of climb cueing methodology and decision logic to provide a smooth transition between each cue under appropriate circumstances. A 3D conformal symbology is designed using the Blender software, a basic simulation environment is created in Unreal Engine, and several desktop simulations are performed in the MATLAB/Simulink environment using pilot models. The primary objective of these studies is to lay the groundwork for future pilot-in-the-loop simulations by designing a framework that could potentially integrate this cueing method into a simulator environment where the cues are presented to the pilot as a 3D conformal symbology set using a Heads-Up Display (HUD). This preliminary work is intended to enhance the potential effectiveness of the pilot's cueing system in hostile and degraded visual environments once actual testing and implementation are underway.

NOTATION

Symbols

H_O	Obstacle Height, ft
R_H	Radius of the sphere surrounding the helicopter, ft
t	time, s
$D(t)$	Closing deceleration on the obstacle, ft/s^2
$V(t)$	Closing velocity on the obstacle, ft/s
$Z(t)$	Distance from an obstacle, ft
τ	time-to-collision (or time-to-contact), s
$\dot{\tau}$	rate of change of τ
τ_m	margin value of τ, s
$\dot{\tau}_m$	margin value of $\dot{\tau}$

Acronyms

DVE	Degraded Visual Environment
HAT	Height Above Terrain
HUD	Heads-Up Display
LTI	Linear Time-Invariant
NDI	Nonlinear Dynamic Inversion
ODE	Ordinary Differential Equation
ROC	Rate of Climb
SA	Situational Awareness

INTRODUCTION

Obstacle avoidance is a widely studied problem for different types of controllable dynamic systems. It has been solved over the years using many different methods: optimal trajectory generation (Ref. 1), panel method-based path planning (Ref. 2), pilot cueing (Ref. 3), and others (Refs. 4–9).

Binet and Rakotomamonjy (Ref. 3) developed an obstacle avoidance methodology using the Tau theory (Ref. 10), which was used to establish haptic cueing by generating force bias on the lateral cyclic. Inspired by this work (Ref. 3), a visual cueing method based on the Tau theory (Ref. 10) for obstacle avoidance was proposed in (Ref. 11). This study presented a method to generate a bank angle cue for a pilot to make a coordinated turn away from the obstacle and safely change the helicopter's trajectory to avoid a collision. In this method, the altitude and speed of the rotorcraft are maintained and the height of the obstacle is assumed to be infinite. Therefore, this method is limited to the 2D plane. However, additional adjustments are required to extend the method to 3D space.

Padfield (Ref. 12) states that pilots have three options when approaching obstacles. They can either turn away from the obstacle, climb over the obstacle, or stop before reaching the obstacle. For time-critical missions, stopping should be the last option to complete the mission in time. Therefore, in DVE conditions, in situations where the bank angle or rate of climb command exceeds the helicopter's limits, the pilot may be advised to decelerate to reduce the load on the helicopter or the engine torque. For this purpose, this paper presents a visual cueing method that combines all three options.

METHODOLOGY

An algorithm with three guidance methods and a logic that provides a smooth transition between them, allowing the pilot to avoid obstacles in DVE conditions, has been developed to increase safety in low altitude, hostile environments. The bank angle guidance method defined in (Ref. 11) was designed to avoid the obstacle in the 2D plane only. In addition to bank angle guidance, deceleration guidance, rate of climb guidance that allow obstacle avoidance in 3D space, and the decision logic that combines them are explained in this section.

Bank Angle Guidance

The Tau theory (Ref. 10) is used in the development of the algorithm to generate bank angle guidance. The geometric approach is illustrated in Figure 1. In (Ref. 11), the algorithm and the notations are described in detail.

In this algorithm, an obstacle of any shape is surrounded by a red circle with radius R_O and center O. There is a safety bubble outside the obstacle, shown as a green circle with a radius of R_S. This is one of the design parameters whose value can be set via extensive simulations for a successful avoidance. The helicopter is also inside a black circle with radius R_H and has center C, which is the center of gravity of the helicopter.

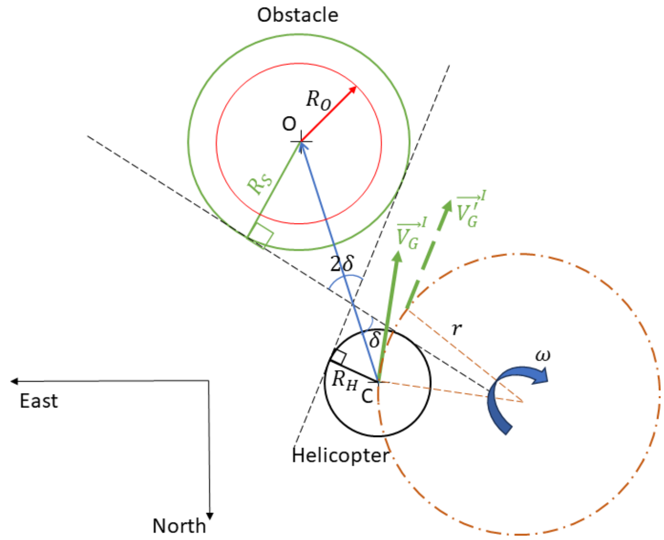

Figure 1. Visualization of the geometric approach for obstacle avoidance (Ref. 11)

Three angle definitions are used to build this algorithm. One is χ, the heading angle, which indicates the direction of the helicopter's ground speed, which does not include the vertical speed. It can be seen as the green solid arrow as V_G in Figure 1. Next is γ, which is the argument of the vector drawn from the helicopter's center of gravity to the center of the obstacle in the inertial frame. The other is δ, which is half the angle between two intersecting tangent lines between the helicopter and the safety bubble, as shown in Figure 1.

The goal is to clear the obstacle by making a coordinated turn until the ground velocity and the tangent line between the helicopter and the safety bubble are parallel to each other. The pilot is expected to perform a turn maneuver to follow the brown dash-dot-dash line shown in Figure 1.

To calculate the time-to-collision estimate, known as τ, the distance over velocity formulation is used (Ref. 10). The reaction distance is calculated as the distance between the centers of the obstacle and the bubble minus their radii. The time-to-collision is estimated using this reaction distance over the ground velocity component parallel to the line of sight from the helicopter to the obstacle. The required turn rate is determined using the time-to-collision estimate.

The location of the obstacle with respect to the helicopter's trajectory is determined by the relationship between χ, γ, and δ. In addition, how much angle to turn in a certain amount of time is also calculated using these angles. In this method, the direction of the turn rate is chosen according to the smallest turn rate.

After the turn rate is found, the bank angle cue can be found. The bank angle cue begins to be shown to the pilot when the estimated time-to-collision is less than a threshold time, τ_m (margin value of the τ), chosen after performing the sensitivity analysis described in (Ref. 11). This is the second design parameter to be selected. This threshold time can also be translated as the threshold distance at which the bank angle cue begins to be displayed. However, in this study, instead of displaying the visual cues according to the threshold distance, the threshold time, τ_m, is used to start displaying the cues.

In (Ref. 11), the performance of the method is tested by performing sensitivity analysis to different τ_m values, assuming sufficient initial distance when approaching the obstacles, changing the size of the obstacles, and changing the position of the obstacles with respect to the helicopter's trajectory. The desktop simulations are performed in the MATLAB/Simulink environment. The Linear Time-Invariant (LTI) model used in the simulations was extracted from the FLIGHTLAB® generic helicopter model at 80 knots, zero sideslip, and forward flight trim condition. These initial simulations were performed with simulated pilot models representing a student pilot and an experienced pilot. This allowed the method to be tested on a variety of pilot skill levels as they represented the two extremes. The pilot models based on the crossover model (Refs. 13, 14) were used to give commands. Details about the pilot models can be found in (Ref. 11). It is found that the best performance of this method can be obtained when the cue is generated 10 seconds before the predicted collision (τ_m = 10 s) and the safety bubble around the obstacle has an adaptive radius that changes with the radius of the obstacle as explained in (Ref. 11). The table of required bubble radii can be found in (Ref. 11).

Rate of Climb Guidance

Similarly, the rate of climb guidance algorithm is developed based on the Tau theory (Ref. 10). The illustration is given in Figure 2.

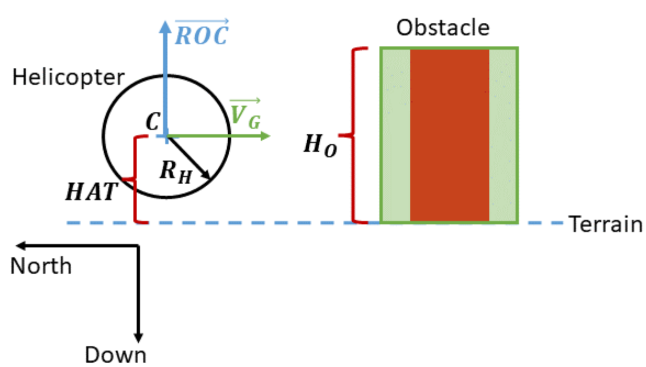

Figure 2. Side view of the visualization of the geometric approach for obstacle avoidance (Ref. 11)

Figure 2 is a side view of Figure 1. In 3D space, it is assumed that the helicopter is inside a sphere with radius R_H and the obstacle with any shape is inside a cylinder with radius R_O and height H_O. Figure 2 shows the side view of the cylinder outside the obstacle as a red rectangle and the safety bubble extruded to the height of the obstacle as a green rectangle. The radius of the safety bubble is determined by extensive simulations as described in (Ref. 11).

The rate of climb guidance is calculated from the vertical distance between the height above terrain (HAT) of the lowest point of the sphere surrounding the helicopter and the highest point of the obstacle, which is the height of the cylinder outside the obstacle. The calculation of the rate of climb guidance is given in Eq. 1.

$$ROC_{CUE} = \frac{H_O - (HAT - R_H)}{\tau} \quad (1)$$

Time-to-collision (τ) is calculated as described in (Ref. 11), which is Eq. 2.

$$\tau = \frac{D_{react}}{|\vec{V_G}^I| cos(\chi - \gamma)} \quad (2)$$

where D_{react} is the distance from an obstacle, also defined as $Z(t)$ in this paper, $\vec{V_G}^I$ is the ground velocity of the helicopter, χ is the heading angle, and γ is the half the angle between two intersecting tangent lines between the helicopter and the safety bubble, shown in Figure 1.

To determine the necessary safety margin above the obstacle for the rate of climb guidance, a series of sensitivity analyses are performed, similar to those performed for the bank angle guidance investigation, except that τ_m, the pilot model, and the relative location of the obstacle with respect to the helicopter's trajectory are held constant. In the sensitivity analysis simulations, the rate of climb is followed while maintaining the forward speed, bank angle, and sideslip. τ_m is kept at 10 seconds as determined in (Ref. 11). Only the student pilot model is used to determine the largest safety margin that would be required. All obstacles are centered on the trajectory of the helicopter. It is assumed that there is sufficient initial distance when approaching the obstacles. Finally, R_H is set to 150 ft in these analyses and the HAT of the helicopter is at 150 ft so that the vertical distance between the lowest point of the sphere around the helicopter and the highest point of the obstacle is always the height of the obstacle.

The sensitivity analyses are performed in the MATLAB/Simulink environment using both the LTI model and the nonlinear model. The LTI model used in the simulations is extracted from the FLIGHTLAB® generic helicopter model at 70 knots, zero sideslip, and forward flight trim conditions. The forward speed is selected according to the best climbing performance speed on the power curve of this generic helicopter in out-of-ground effect, sea level, and standard atmospheric conditions, shown in Figure 3.

Sensitivity analyses are performed using obstacles with radii of 50 ft, 100 ft, 150 ft, 300 ft, 500 ft, 1000 ft, and 2000 ft and heights of 50 ft, 100 ft, 150 ft, 300 ft, 500 ft, 1000 ft, and 2000 ft. As a result, there is no pattern for a safety margin. Therefore, no safety margin is implemented in the vertical direction. However, it is observed that if the height of the obstacle is less than 150 ft, the obstacle is cleared in all cases.

Figures 4 and 5, respectively, show LTI and nonlinear model simulation results for a 50 ft radius, and 150 ft high obstacle in isometric and side views.

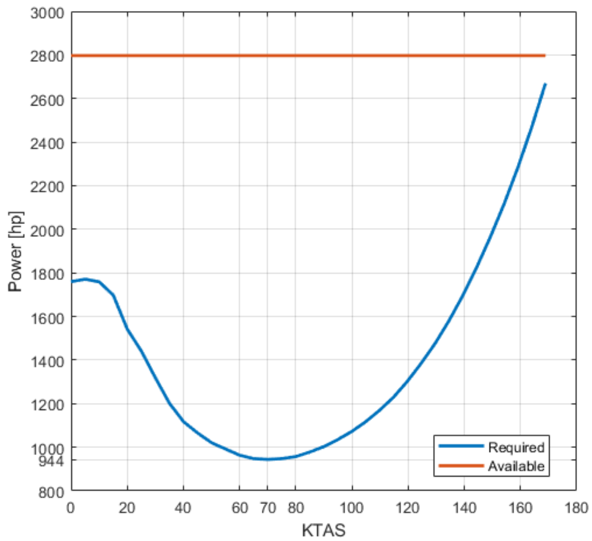

Figure 3. Power curve of the generic helicopter model at sea level, out-of-ground effect, standard atmospheric conditions

Deceleration Guidance

The study by Lee (Ref. 10) investigates the effect of time-to-collision information on visual control of braking in traffic, which concludes that the easiest type of information to control braking is visually perceived time-to-collision information, rather than distance, speed, or deceleration/acceleration and that the driver maintains a safe margin value of the derivative of the time-to-collision ($\dot{\tau}_m$) while controlling braking. Therefore, the deceleration guidance algorithm, which calculates the deceleration trajectory while keeping $\dot{\tau}$ constant, is based on this study. The derivation of the deceleration trajectory is explained in detail in the appendix of (Ref. 10). As described in (Ref. 10), the time to collision is defined by Eq. 3.

$$\tau = \frac{Z(t)}{V(t)} \tag{3}$$

The time derivative of τ becomes Eq. 4.

$$\dot{\tau} + 1 = \frac{D(t)Z(t)}{V(t)^2} \tag{4}$$

where $V(t) = -d(Z(t))/dt$ and $D(t) = d^2(Z(t))/dt^2$. It is assumed that the deceleration starts at $t = 0$, therefore, $V(0)$ is the speed at which the deceleration starts, and $Z(0)$ is the distance from the obstacle at $t = 0$.

The deceleration trajectory is found by solving Eq. 4 with $\dot{\tau} = \dot{\tau}_m$, which is given in Eq. 5.

$$V(t) = V(0)\left(1 + \frac{\dot{\tau}_m V(0) t}{Z(0)}\right)^{-1-\frac{1}{\dot{\tau}_m}} \tag{5}$$

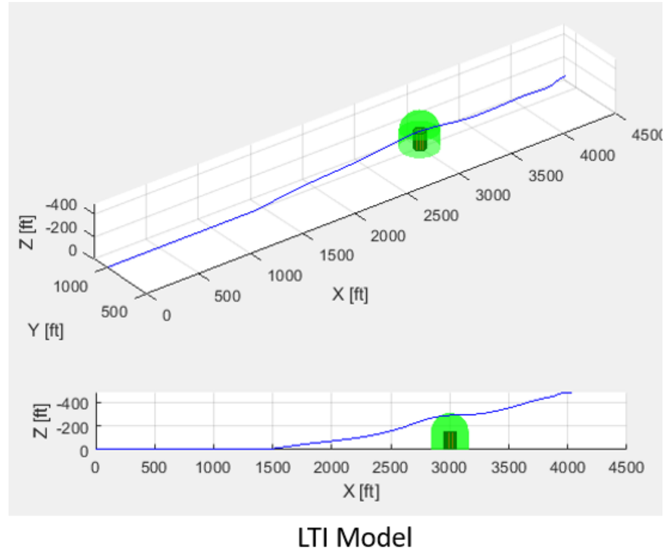

Figure 4. Obstacle avoidance LTI model simulation using the rate of climb guidance - 50 ft radius 150 ft high obstacle

Figure 6 shows the deceleration trajectory for different safe margin values of $\dot{\tau}$ ($\dot{\tau}_m$) from -0.5 to -0.1. Since the slowest deceleration occurs when $\dot{\tau}_m = -0.1$, $\dot{\tau}_m$ is chosen as -0.1 to avoid the abrupt changes in the cue.

After generating the deceleration trajectory, it is transformed into a pitch angle guidance using nonlinear dynamic inversion (NDI) as described in (Ref. 15).

LTI models are extracted at different forward speeds, and zero sideslip trim conditions using FLIGHTLAB®'s generic helicopter model. The following Eq. 6 is the approximate LTI model.

$$\dot{u} = X_u u - g\theta \tag{6}$$

where u is the velocity in the X direction of the body frame, θ is the pitch angle, and g is the gravitational acceleration. Figure 7 shows the block diagram of the transition from the deceleration trajectory to the pitch angle guidance.

A first-order command model is used to designate the desired response of the system, which is given in Eq. 7, where T is the time constant. The time constant T is selected as 1 second for this application.

$$G_{ideal}(s) = \frac{1}{Ts+1} \tag{7}$$

A PI controller is used for error compensation of the generated deceleration trajectory, with the proportional gain K_P set to 0.3 and the integral gain K_I set to 0.13.

Decision Logic

Based on desktop simulations performed to test the performance of the individual bank angle and rate of climb guidance algorithms, the decision logic is implemented to prevent

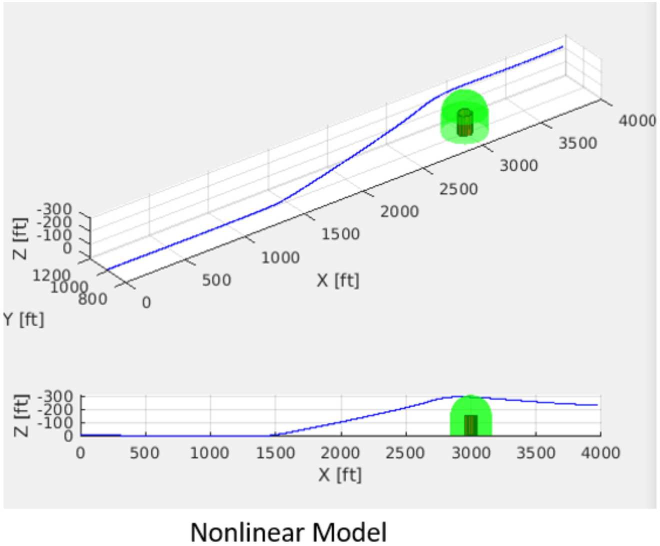

Figure 5. Obstacle avoidance nonlinear model simulation using the rate of climb guidance - 50 ft radius 150 ft high obstacle

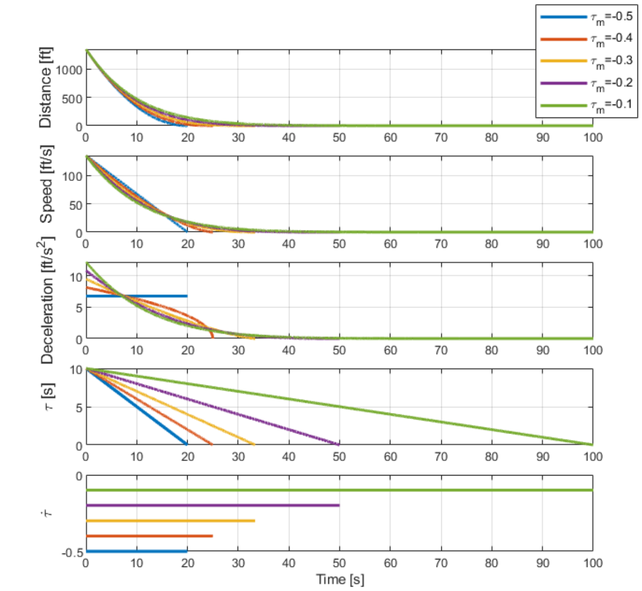

Figure 6. Deceleration trajectory for different $\dot{\tau}_m$

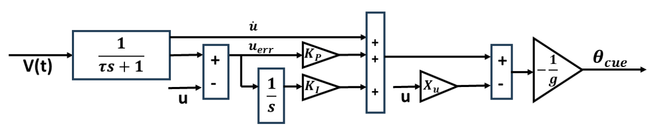

Figure 7. Pitch angle guidance generation using NDI

the helicopter from reaching its limits while safely avoiding the obstacle.

The need to generate the rate of climb and deceleration guidance comes from the findings in (Ref. 11), where it is stated that there is a need for alternative guidance methods for very high bank angle guidance, although it is a very effective way of obstacle avoidance. Therefore, the logic was mainly built around the bank angle guidance algorithm. In the desktop simulations, it is observed that if the vertical distance between the lowest point of the sphere surrounding the helicopter and the highest point of the obstacle is less than 150 feet, the obstacles can be avoided when τ_m is 10 seconds. Therefore, the first step is to check the vertical distance. If it is less than 150 feet, the pilot is shown the rate of climb cue while maintaining the helicopter's speed at 70 knots. Generating the rate of climb cue does not change the initial trajectory, which is important for time-sensitive missions. However, if the vertical distance is greater than 150 feet, the bank angle cue is used to clear the obstacle. Therefore, the second step must ensure that the helicopter does not reach very high bank angles. Since the load factor is 2 when the bank angle is 60° and it is seen in the desktop simulations that the generic helicopter model that is used in the simulations cannot make turns with a bank angle higher than 60°, in the second checkpoint the magnitude of the bank angle cue is examined. If it reaches 60°, the deceleration cue is displayed along with the bank angle cue until it becomes less than 60°. This algorithm is developed for speeds higher than 60 knots. For low-airspeed flight (<= 40 knots) different obstacle avoidance algorithms should be used.

The logic is summarized in Figure 8. This flowchart combines all three algorithms to provide a safe obstacle avoidance methodology. This logic can be adapted according to the requirements determined after the pilot-in-loop tests.

DESCRIPTION OF 3D CONFORMAL SYMBOLOGY SET

This research presents an approach to rotorcraft cueing that integrates time with spatial visualization to provide pilots with an intuitive and comprehensive understanding of their immediate flight environment and trajectory. The goal is to provide pilots with a dynamic and predictive view of their environment, enabling them to make informed decisions quickly and safely by adopting a 4D perspective. This approach is particularly relevant in DVE conditions. Since the obstacle avoidance guidance algorithm is designed to be implemented as a 4D conformal pilot cueing system, a 3D conformal symbology set is required. In this paper, three visual cues have been proposed comprising all the guidance algorithms to be tested in the GaTech high-fidelity, fixed-base rotorcraft flight simulator.

Bank Angle and Deceleration Cue

The bank angle cue and the deceleration cue symbologies, which are translated into the symbology of the pitch angle cue, are inspired by standard flight directors. While the cue is represented by two wing-like bars connected by a semicircle on top of each other, the helicopter's actual bank and pitch angles are represented by a bar with a circle in the center of the bar. The pilot ensures that the obstacle avoidance cue is followed by keeping the attitude indicator bar within the cue indicator

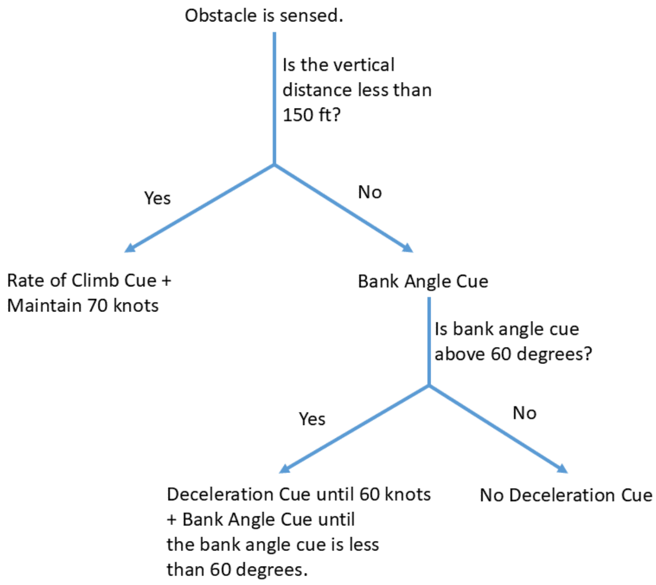

Figure 8. Decision making flow chart

bar. When the bank angle cue is generated, the wing-like bars tilt left or right, and when the pitch angle cue is generated, they move up or down together. If the pilot manages to keep the bar inside the cue indicator bar, the cue will be followed successfully. Both the cue and the actual attitude indicators are placed in the center of the HUD, just in front of the pilot's eye level. A screenshot of the cue indicator design in Blender is shown in Figure 9 and a screenshot of the bank angle and pitch angle indicator design in Blender is shown in Figure 10.

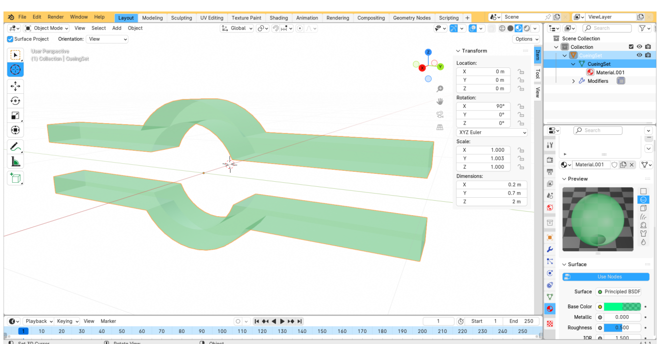

Figure 9. Bank angle and deceleration cue indicator design shown in Blender

Rate of Climb Cue

The rate of climb cue symbology uses a hollow arrow pointing up in the upper left corner of the HUD. This indicates a maximum climb rate of 4000 fpm. As the helicopter gains climb rate, the hollow arrow fills with a vertical bar, in other words, the helicopter's actual climb rate value is displayed as a bar that fills the hollow arrow indicating the rate of climb cue. A screenshot of the rate of climb cue indicator design

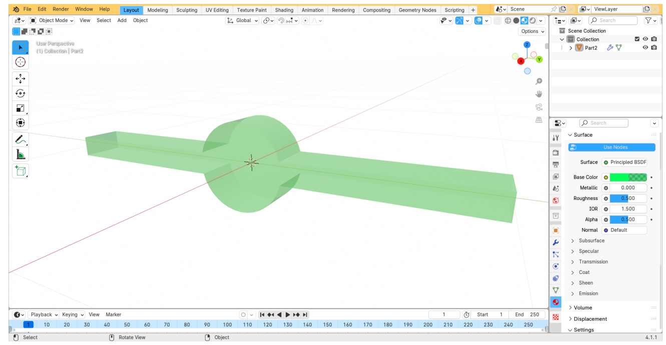

Figure 10. Bank angle and pitch angle indicator design shown in Blender

and the actual rate of climb indicator in Blender is shown in Figure 11.

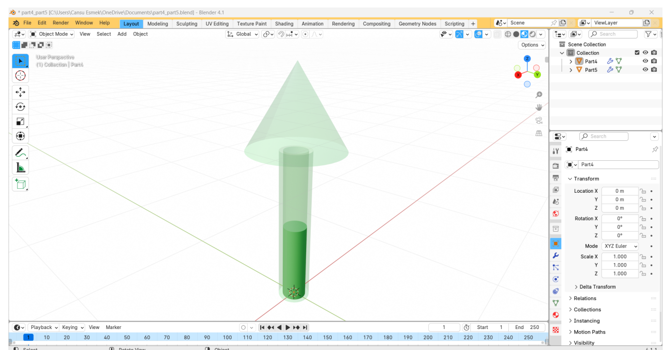

Figure 11. Rate of climb cue indicator design and the actual rate of climb indicator shown in Blender

Glass Dome

The glass dome cue indicates a safety bubble around the obstacle, extruded as high as the obstacle, and a hemisphere of the same radius with the safety bubble on top. It is inspired by the study (Ref. 16). The glass dome appears on the outside of the obstacle to be avoided by the avoidance algorithm. A screenshot of the glass dome cue indicator design in Blender is shown in Figure 12.

SIMULATION

Environment in Unreal Engine

The simulation environment for initial tests is created in Unreal Engine 5.1 and Unreal Engine 4.27 environment. The simulation environment consists of cylindrical obstacles of various sizes, realistic terrain imported from the Cesium plugin, and a UH60 helicopter model found on the Epic Games Marketplace.

Desktop Simulations

In order to test the performance of the methodology in terms of obstacle avoidance and mission completion within the

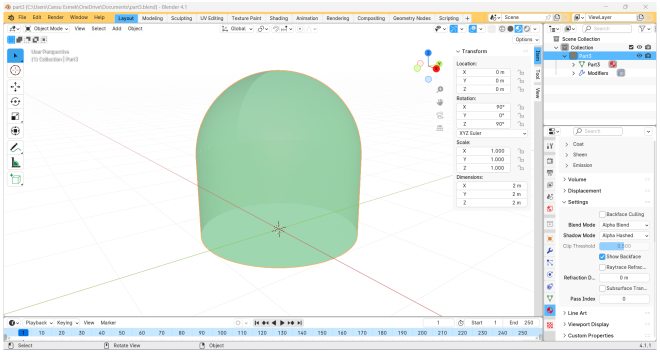

Figure 12. Glass dome design shown in Blender

specified time interval capability, several desktop simulations are performed. Both the LTI model extracted using the FLIGHTLAB® generic helicopter model and the nonlinear model itself are used for this purpose. The simulations are performed in the MATLAB/Simulink environment. Pilot models representing experienced and inexperienced pilots are used to complete the simulations. The pilot models based on the crossover model (Refs. 13, 14) are used to give commands. The transfer function of the pilot model is given in Eq. 8, where K_p is the pilot gain, T_L, and T_I are lead-lag time constants and τ^e is the time delay. Since the same pilot models are used in this study with the (Ref. 11), details on the pilot models can be found in (Ref. 11).

$$Y_p(s) = K_p \frac{1+T_L s}{1+T_I s} . e^{-\tau_e s} \tag{8}$$

The architecture of the pilot model consists of four input channels. The collective channel tracks the rate of climb. The pilot model finds the appropriate collective input. In the pedal channel, zero lateral acceleration is achieved for a forward speed greater than 60 knots. The pilot model finds the required pedal input for zero lateral acceleration. In the longitudinal cyclic channel, the pitch angle cue is followed. The pilot model finds the required longitudinal cyclic input for that pitch angle. In the lateral cyclic channel, the pilot model follows the bank angle command. A basic SAS with zero time delay, zero noise, and unity transfer functions for SAS sensors and actuators is implemented to increase stability during simulations. Lead-lag time constants and time delay are kept at zero except for the inner loops in the four input channels. Figure 13 shows the controllers.

Simulation Results and Discussion

Desktop simulations start with 80 knots forward flight trim conditions with zero sideslip. In all simulations, the mission is plotted as the helicopter moves from $(x,y) = (0,1000)[ft]$ coordinates in the inertial frame at 150 ft altitude to the target point $(x,y) = (10000,1000)[ft]$ coordinates in the inertial frame at 150 ft altitude. In the simulations, the number, size, and location of obstacles are kept as variables, resulting in different terrain scenarios. The results of a sample simulation

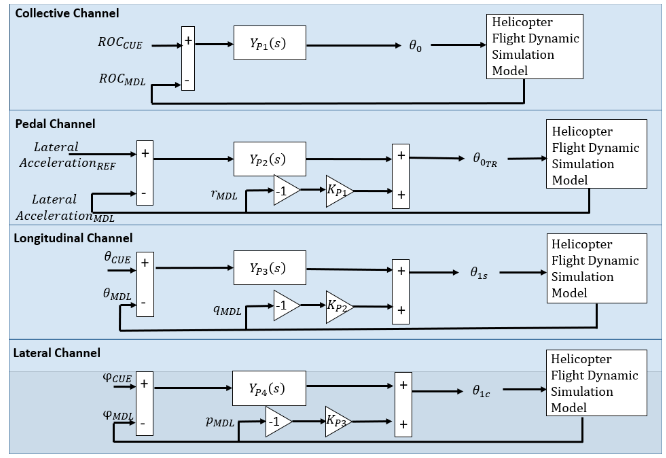

Figure 13. Pilot model architecture

performed using the nonlinear model are shown from the top, side, and isometric views in Figures 14, 15, and 16, respectively.

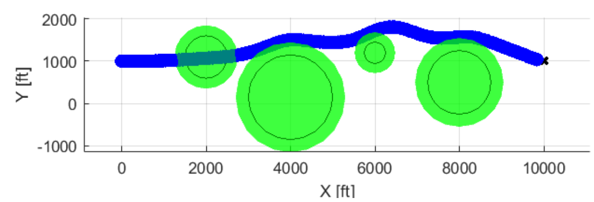

Figure 14. Top view of the helicopter's trajectory

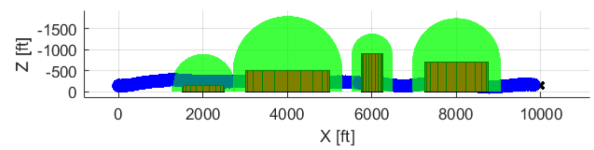

Figure 15. Side view of the helicopter's trajectory

For this simulation, the obstacle specifications are given in Table 1.

The bank angle cue and the helicopter's actual bank angle and lateral cyclic values are shown in Figure 17. Because the bank angle cue did not exceed 60 degrees in this simulation, the helicopter maintained 80 knots throughout the mission, except during a climb maneuver while avoiding the fourth obstacle, where the helicopter slowed to and maintained a forward speed of 70 knots. Similarly, the pitch angle cue, the helicopter's actual pitch angle, and the longitudinal cyclic can be seen in Figure 18 and the rate of climb cue, the helicopter's actual rate of climb, and the collective input are shown in Figure 19.

One can find the lateral acceleration and compensating pedal input during this simulation in Figure 20.

In these simulations, it is seen that the mission could be com-

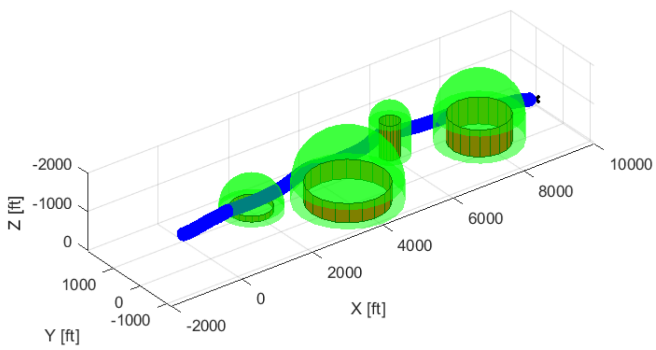

Figure 16. Isometric view of the helicopter's trajectory

Table 1. Obstacle's Description

Radius [ft]	Height [ft]	Location (x,y) [ft]
1000	500	(4000, 150)
250	900	(6000, 1200)
750	700	(8000, 500)
500	150	(2000, 1100)

pleted without hitting the obstacle and close to the target mission duration most of the time. Therefore, the methodology is ready to be tested in the simulator environment with the pilots. However, as it is seen that the results are highly dependent on the pilot models, the results are not conclusive until the pilot-in-the-loop tests are conducted.

The desktop simulations have shown that the methodology works, but the pitch angle cue is highly variable, so the transition from deceleration trajectory to pitch angle guidance should be fine-tuned before implementation in the simulator. A fluctuating pitch angle cue not only results in an oscillating forward speed but also makes it more difficult to follow the rate of climb cue without descending.

As concluded in (Ref. 11), the bank angle cue works with high accuracy and it promises great safety together with the rate of climb cue and the deceleration cue, which makes it possible to avoid obstacles without exceeding the helicopter's limits.

CONCLUSIONS

This study proposes a deceleration and rate of climb guidance methodology and decision logic to provide a smooth transition between each cue under appropriate circumstances, in addition to the bank angle guidance methodology explained in (Ref. 11). With this study, the method has been transformed into a possible 3D conformal symbology using the Blender software, and a basic simulation environment is created in Unreal Engine to design the test environment and test scenarios. The results of the various desktop simulations performed in MATLAB/Simulink using the Flighlab generic helicopter model are discussed. The findings are listed below:

1) The mission could be completed without hitting the obstacle and close to the target mission duration most of the time.

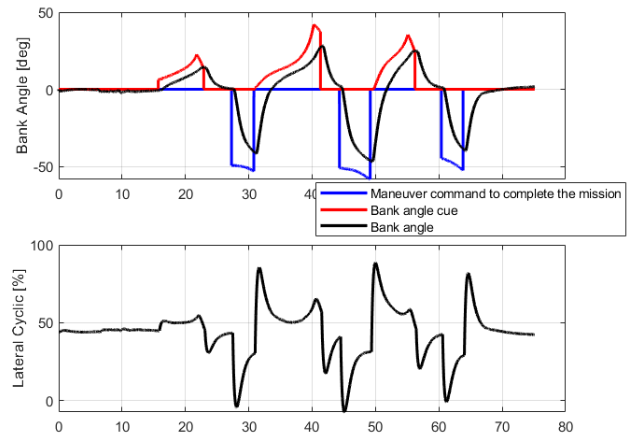

Figure 17. Bank angle cue and the lateral channel

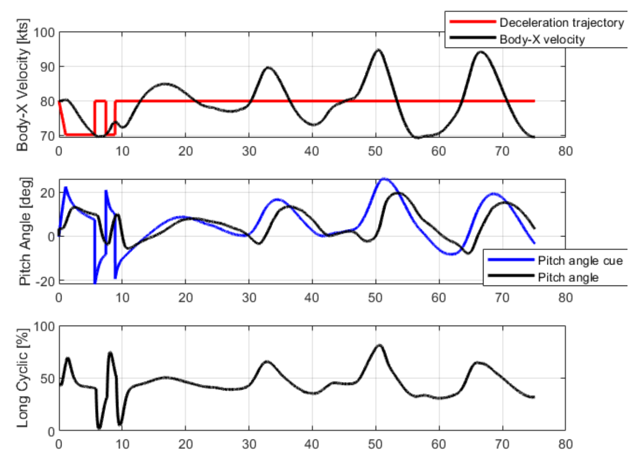

Figure 18. Pitch angle cue and the longitudinal channel

Therefore, the methodology is ready to be tested in the simulator environment with the pilots.

2) The desktop simulations have confirmed that the methodology works, but the pitch angle cue is highly variable, so the transition from deceleration trajectory to pitch angle guidance should be fine-tuned before implementation in the simulator. A fluctuating pitch angle cue not only results in an oscillating forward speed but also makes it more difficult to follow the rate of climb cue without descending.

3) As concluded in (Ref. 11), the bank angle cue works with high accuracy and it promises great safety together with the rate of climb cue and the deceleration cue, making it possible to avoid obstacles without exceeding the helicopter's limits.

4) Since the simulation results are highly dependent on the pilot models, the results are not conclusive until the pilot-in-loop tests are performed.

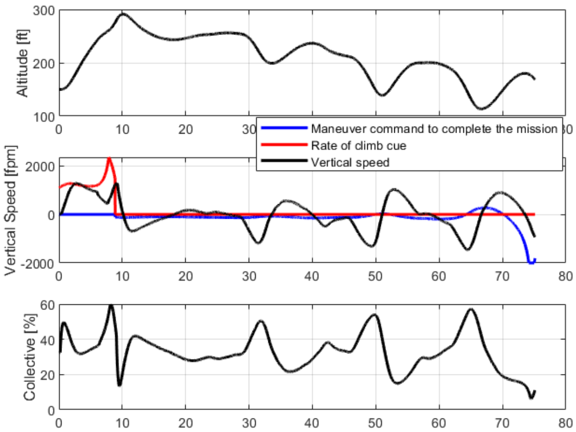

Figure 19. Rate of climb cue and the collective channel

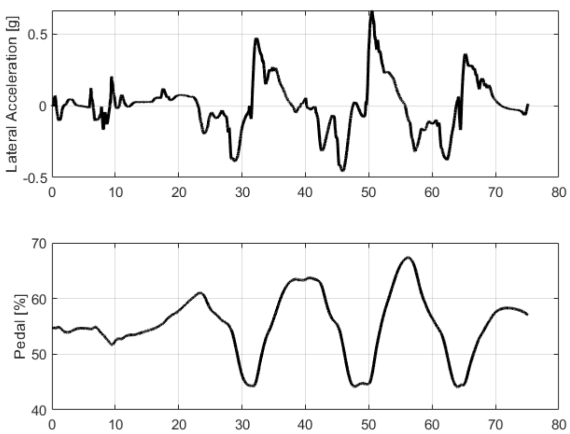

Figure 20. Lateral acceleration and the pedal channel

FUTURE WORK

In future work, the visual cueing method will be implemented in the GaTech's high-fidelity fixed-base rotorcraft flight simulator, and pilot-in-the-loop simulations will be conducted to further refine the parameters and feasibility of this method.

Author contact: Ceren Cansu Esmek cesmek3@gatech.edu, Rahul Tauro-Padival rahulpadival@gatech.edu, J.V.R. Prasad jvr.prasad@gatech.edu, & Karen M. Feigh karen.feigh@gatech.edu

ACKNOWLEDGMENTS

This research was partially funded by the U.S. Government under Cooperative Agreement No. W911W6-21-2-0001. The U.S. Government is authorized to reproduce and distribute reprints for Government purposes notwithstanding any copyright notation thereon. The views and conclusions contained in this document are those of the authors and should not be interpreted as representing the official policies of position, either expressed or implied, of the U.S. Army Combat Capabilities Development Command (DEVCOM), Aviation & Missile Center (AvMC), or the U.S. Government.

REFERENCES

1. Kang, K., Prasad, J., and Dhingra, M., "Simulation Evaluation Of An Adaptive Optimal Multiple Obstacle Avoidance Algorithm For Autonomous UAVs," Proceedings of the American Helicopter Society 67th Annual Forum, 2011.

2. Unal, Z., and Yavrucuk, I., "Panel-Method-Based Path Planning for eVTOL in Urban Environment," Proceedings of the Vertical Flight Society 77th Annual Forum, 2021.

3. Binet, L., and Rakotomamonjy, T., "Using Haptic Feedbacks For Obstacle Avoidance In Helicopter Flight," Proceedings of the 6th European Conference for Aeronautics and Space Sciences (EUCASS), 2015.

4. Rakotomamonjy, T., Binet, L., and Müllhäuser, M., "ONERA-DLR Joint Research On Tactile Cueing For Reactive Obstacle Avoidance Dedicated To Low Speed Helicopter Maneuvers," Proceedings of the 44th European Rotorcraft Forum, 2016.

5. Walko, C., and Müllhäuser, M., "Design Of A Haptic Obstacle Avoidance For Low-Speed Helicopter Operations Using Active Sidesticks," *The Aeronautical Journal*, 2023, pp. 1–17.

6. Godfroy-Cooper, M., Miller, J. D., Szoboszlay, Z., and Wenzel, E. M., "3D-Sonification for Obstacle Avoidance in Brownout Conditions," Proceedings of the 73th American Helicopter Society Annual Forum Technology Display, 2017.

7. Godfroy-Cooper, M., Miller, J. D., Bachelder, E., and Wenzel, E. M., "Isomorphic Spatial Visual-Auditory Displays For Operations In DVE For Obstacle Avoidance," Proceedings of the 44th European Rotorcraft Forum, 2018.

8. Miller, J. D., Godfroy-Cooper, M., and Wenzel, E. M., "ARSAD: An Augmented-Reality Spatial Auditory Display for Obstacle Avoidance for all Phases of Flight," Proceedings of the 74th American Helicopter Society Annual Forum Technology Display, 2018.

9. Miller, J. D., Godfroy-Cooper, M., and Szoboszlay, Z. P., "Augmented-Reality Multimodal Cueing for Obstacle Awareness: Towards a New Topology for Threat-Level Presentation," Proceedings of the 75th American Helicopter Society Annual Forum Technology Display, 2019.

10. Lee, D. L., "A Theory of Visual Control of Braking based on Information about Time-to-Collision," *Perception*, Vol. 5, 1976, pp. 437–459.

11. Kwon, J., Esmek, C., Tauro-Padival, R., Prasad, J., and Feigh, K., "4D Conformal Pilot Cueing for Rotorcraft Army Operational Scenarios," Proceedings of the Vertical Flight Society 80th Annual Forum Technology Display, 2024.

12. Padfield, G. D., "The Tau of Flight Control," *The Aeronautical Journal*, Vol. 115, 2011, pp. 521–556.

13. McRuer, D. T., and Jex, H. R., "A Review of Quasi-Linear Pilot Models," *IEEE Transactions on Human Factors in Electronics*, Vol. HFE-8, 1967, pp. 231–249.

14. Friesen, D., Pavel, D. M., Borst, C., Masarati, P., and Mulder, M., "Pilot Model Development And Human Manual Control Considerations For Helicopter Hover Displays," Proceedings of the 45th European Rotorcraft Forum, 2019.

15. Saetti, U., Rogers, J., Alam, M., and Jump, M., "Tau Theory-Based Flare Control in Autonomous Helicopter Autorotation," *Aerospace*, Vol. 11,33, 2024.

16. Peineckea, N., Chignolab, A., Schmida, D., and Friedlb, H., "The Glass Dome: Low-Occlusion Obstacle Symbols for Conformal Displays," *SPIE*, Vol. 9839 983907, 2016.